symmetry

IMPACT FACTOR 2.2

CITESCORE 5.4

Article

Scalar Greybody Radiation of "NRIGP" Black Hole

Sara Kanzi

MDPI

https://doi.org/10.3390/sym17010042

symmetry

MDPI

Article

Scalar Greybody Radiation of "NRIGP" Black Hole

Sara Kanzi

Faculty of Engineering, Final International University, North Cyprus via Mersin 10, Kyrenia 99320, Turkey; sara.kanzi@final.edu.tr

Abstract: The present paper investigates the greybody radiation of a general metric including the significant black hole parameters. The fraction of Hawking radiation (HR) that succeeds in achieving infinity is known as "greybody radiation" or transmission probability. In this study, the focus is on the black hole parameters by which greybody radiation could be affected, such as electric and magnetic charges "e" and "g", respectively, cosmological constant "Λ", and Taub-Nut "l". In this regard, we use the nonrotating form of the improved Griffiths–Podolsk (NRIGP) metric which contains the factors "Λ, l, e, g", all in a single metric. This study allows us to observe the behavior of the scalar perturbation and greybody radiation of each indicated parameter in the presence of the other variables. The spacetime around the black hole behaves as a barrier for particles, and the greybody factor strongly depends on the black hole potential barrier. Therefore, we first studied the scalar perturbation and evaluated the actions of the effective potential by the regarded parameters. The depicted figures for variables such as magnetic charge "g" confirm the consistency between the effective potential and the greybody factor. In this area of study, symmetry plays an essential but hidden role. In the current study, we also consider that all the particles around a black hole have the same symmetry.

Keywords: Hawking radiation; greybody factor; effective potential; Klein-Gordon equation

1. Introduction

Classically, a physical body that absorbs complete incident electromagnetic radiation is known as the black body, a body that also emits maximized thermal radiation. A semi-black body that does not perfectly absorb and emit radiation is called a greybody and is measured between zero and one.

In the quantum gravity framework, black holes can also emit from their event horizon, known as Hawking radiation, which was proposed by S.W. Hawking in 1974 [1,2]. Some pairs of particles near the horizon might be disjoint, as shown in Figure 1; thus, one with negative energy falls into the black hole, and the other one with positive energy escapes to create Hawking radiation. However, a fraction of the Hawking radiation an observer receives at infinity is called the greybody factor, which differs from an initial black hole spectrum. Therefore, the greybody factor of the black hole is a parameter that expresses the deviation of Hawking radiation from pure blackbody radiation and depends on the frequency.

Academic Editor: Branko Dragovich

Received: 3 December 2024
Revised: 24 December 2024
Accepted: 27 December 2024
Published: 29 December 2024

Citation: Kanzi, S. Scalar Greybody Radiation of "NRIGP" Black Hole. *Symmetry* **2025**, *17*, 42. https://doi.org/10.3390/sym17010042

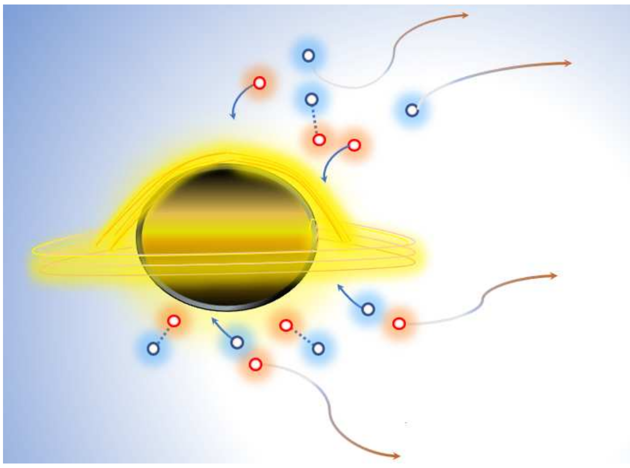

Figure 1. A simple schema of Hawking radiation when some pairs of particles around the horizon are separated, some with negative energy fall into the black hole, and some escape as Hawking radiation. The blue and red colors differentiate the particles of a pair.

Greybody radiation can also be used as a scale to estimate black hole evaporation. The difference between the black hole's black body and greybody is that the black body factor is defined by the possibility of the particles being created in the area of a horizon, and the greybody factor is the probability that the particles infiltrate the potential barrier (nontrivial spacetime surrounding a black hole) and escape to infinity. Potential barriers on the outer side of the horizon act as a filter that depends on the frequency; some radiations reflect into the black hole, and some transmit to infinity. Black hole dissipation is expressed via linearized wave equations, which, indeed, determine the symmetrical perturbation of the particles in the black hole. Therefore, in black hole geometry, the equation representing particle perturbations can be given as a one-dimensional Schrödinger-form wave equation. There are several techniques and investigations for computing the greybody factor, taking different choices of black hole solutions, such as the evaluation of the scalar field excitations impact on the greybody factor of the Myers–Perry black hole [3], the greybody factor of $5-d$ rotating black hole [4], higher-dimensional black holes with the different cosmological constant in low-frequency regime [5], charged rotating black hole in the frame of quintessential energy [6]; in this context is also [7], in the framework of the Bumblebee gravity model [8,9], in dRGT massive gravity [10,11], in the brane-world black hole [12], and also [13].

The emitted spectrum near the horizon is identical and contains important information about the black hole's physical structure. Therefore, investigating this area could be a promising way to obtain information from the black hole puzzle, and it is still at the center of attention [14–23].

The impact of the significant parameters in the greybody factor is mostly evaluated separately in the literature. Motivated by the above works, in this study, we aim to consider the impression of all important arguments like magnetic and electric charges "g" and "e", cosmological constant "Λ", and NUT parameters "l" in a single metric. For this aim, we consider the nonrotating improved form of the Griffiths–Podolsk (NRIGP) metric introduced by Podolsky and Veratny [24]. The improved form of the Griffiths–Podolsk metric is a complete group of exact black hole spacetimes of algebraic type D, containing any cosmological constant [25]. This class was founded by Debever in 1971 [26], expanded by Plebanski and Demianski in 1976 [27], and then reformulated in a more convenient form by Griffiths and Podolsky in 2005 [28].

The improved form of the metric enables us to investigate and evaluate various properties of a large family of rotating (Kerr), charged (Reissner–Nordstrom), accelerating black holes (Kinnersley–Walker), and cosmological constant (Kottler–Weyl–Trefftz).

In this paper, we restrict ourselves only to the nonrotating and nonacceleration forms of the improved Griffiths–Podolsk metric, which is abbreviated as "NRIGP".

The construction of the paper is as follows; after a brief review of the general improved form of the Griffiths–Podolsk and NRIGP metrics in Section 2, we study the scalar perturbation to derive the effective potential via the $1-d$ Schrödinger-form wave equation by utilizing the massive and charged Klein-Gordon equation in Section 3. In Section 4, we aim to evaluate the greybody radiation of the NRIGP metric via the semianalytic method by taking advantage of the results in Section 3, and, finally, we provide the conclusion in Section 5. Throughout this paper, the signature $(-,+,+,+)$ and geometrized units $C=G=1$ are used.

2. The Improved Griffiths–Podolsk Metric

In this part, we plan to summarize the new metric representation of the complete group of black holes held in the spacetime of the Plebanski–Demianski (they expressed a combination of a large group of Einstein-Maxwell electro-vacuum (algebraic type D) solutions [29], containing Taub-NUT spacetime, Kerr-Newman black hole, and (anti-)de Sitter (AdS) metric) [27]. The Plebanski–Demianski model was boosted by Griffiths and Podolsky as a set of accelerating and rotating charged black holes, including a NUT parameter [28]. In a new improved form in Ref. [25], authors demonstrated the Plebanski–Demianski model in a more convenient form and introduced a modified set of the mass and charge parameters of the Griffiths and Podolsky metric.

The exact black hole solutions such as Schwarzschild and Reissner-Nordström are spherical/axially symmetric and affiliated to a general group of type D spacetime but still do not belong to the Plebanski–Demianski class of solutions. The Plebanski–Demianski solution contains the Kerr–Newman and Kerr–NUT, the Schwarzschild and the Reissner–Nordström, and the acceleration black holes.

This paper also uses the new improved metric of Griffiths and Podolsky containing the cosmological constant [25]. In order to have a more straightforward computation, we consider the nonrotating and consequently nonacceleration cases of the improved form of the Griffiths–Podolsk (NRIGP).

The new improved metric representation found by Griffiths and Podolsky [28,30,31] is given by [25]

$$ds^2 = \frac{1}{\Omega^2}\left(-\frac{1}{\rho^2}(Q - Pa^2 sin^2\theta)dt^2 + \frac{\rho^2}{Q}dr^2 + \frac{\rho^2}{P}d\theta^2 + \frac{B}{\rho^2}d\phi^2 + \frac{2C}{\rho^2}dtd\phi\right) \tag{1}$$

where

$$\begin{aligned} B &= P\sin^2\theta(r^2 + (a+l)^2)^2 - Q(a\sin^2\theta + 4l sin^2\frac{1}{2}\theta)^2\,, \\ C &= 4Ql\sin^2\frac{1}{2}\theta + Qa\sin^2\theta - Pa\sin^2\theta(r^2 + (a+l)^2), \end{aligned} \tag{2}$$

with the following expressions:

$$\Omega = 1 - \frac{a\alpha}{a^2+l^2} r(l + acos\theta)\,,$$
$$\rho^2 = r^2 + (l + acos\theta)^2\,,$$
$$P = 1 - 2(\frac{a\alpha}{a^2+l^2} m - \frac{\Lambda}{3} l)(l + acos\theta) + (\frac{a^2\alpha^2}{(a^2+l^2)^2}(a^2 - l^2 + e^2 + g^2) + \frac{\Lambda}{3})(l + acos\theta)\,,$$
$$Q = \left[r^2 - 2mr + (a^2 - l^2 + e^2 + g^2)\right]\left(1 + ar\alpha\frac{a-l}{a^2+l^2}\right)\left(1 - ar\alpha\frac{a+l}{a^2+l^2}\right) - \frac{\Lambda}{3} r^2 \times$$
$$\left(r^2 + 2alr\alpha\frac{a^2-l^2}{a^2+l^2} + (a^2 + 3l^2)\right), \tag{3}$$

in which parameters m, l, g, e, a, α, and Λ represent the mass, NUT, magnetic charge, electric charge, rotating, acceleration, and cosmological constant factors, respectively.

The electromagnetic field is expressed by Maxwell tensor as F_{ab}, creating a differential electromagnetic four potential 1-form $\mathbf{F} = d\mathbf{A}$, in which 2-form is $\mathbf{F} = \frac{1}{2} F_{\mu\nu} dx^\mu \wedge dx^\nu$, and $\mathbf{A} = A_\mu dx^\nu$, given by

$$\mathbf{A} = -\frac{er + g(l + a\cos\theta)}{r^2 + (l + a\cos\theta)^2} dt + \frac{(er + gl)(a\sin^2\theta + 4lsin^2\frac{1}{2}\theta) + g(r^2 + (a+l)^2)\cos\theta}{r^2 + (l + a\cos\theta)^2} d\phi. \tag{4}$$

Thus, the nonzero components are

$$F_{rt} = \rho^{-4}\Big(e(r^2 - (l + a\cos\theta)^2) + 2gr(l + a\cos\theta)\Big)\,,$$
$$F_{\phi\theta} = \rho^{-4}\Big(g(r^2 - (l + a\cos\theta)^2) - 2er(l + a\cos\theta)\Big)(r^2 + (a+l)^2)\sin\theta\,,$$
$$F_{\phi r} = (a\sin^2\theta + 4l\sin^2\frac{1}{2}\theta)F_{rt}\,,$$
$$F_{\theta t} = \frac{a}{r^2 + (a+l)^2} F_{\phi\theta}. \tag{5}$$

The line element described in Equation (1), is the most general exact Einstein–Maxwell solution of algebraic type D, which includes important physical factors. On the other hand, by considering the noncorresponding parameters to zero, the main subclasses such as Kerr–Newman and other regarded types are recovered; for instance, by assuming $\alpha = a = \Lambda = g = e = 0$ in Equation (1), the Schwarzschild metric is recovered. Considering all the factors in one metric provides us with a great opportunity to evaluate the impacts of each separately alongside other parameters, but also is difficult to compute. Therefore, the evaluation for more convenience should be in different subclasses. In this paper, our concern is for the nonacceleration and nonrotation subclass, namely, the NRIGP metric. To this aim, we consider the Kerr (rotating) parameter "a" as zero, and explicitly the acceleration α dependent terms will disappear from Equations (1)–(3). Thus the NRIGP metric is written

$$ds^2 = -\frac{Q}{\rho^2}(dt - 4lsin^2\frac{1}{2}\theta d\phi)^2 + \frac{\rho^2}{Q}dr^2 + \frac{\rho^2}{P}d\theta^2 + \frac{P}{\rho^2}sin^2\theta(r^2 + l^2)^2 d\phi^2, \tag{6}$$

where the regarded parameters are given by

$$\rho^2 = r^2 + l^2\,,$$
$$P(\theta) = 1 + \Lambda l^2\,,$$
$$Q(r) = \left[r^2 - 2mr + e^2 + g^2 - l^2\right] - \frac{\Lambda}{3} r^4 - \Lambda r^2 l^2. \tag{7}$$

The location of the horizon of the metric equation (1) is derived by solving $Q(r) = 0$, a fourth-order root polynomial. Therefore, the four horizons are designated as the following. (1) The outer and inner black hole horizons at r_h^+ and r_h^-. (2) The cosmological and acceleration (cosmo-acceleration) horizons due to the acceleration α and cosmological constant Λ located at $r_c^{\pm}$, where $+$ and $-$ indicate the outer and inner cosmo-acceleration horizons. To define the roots of the metric function of Equation (1), let us generate $Q(r)$ as

$$Q(r) = I_1 r^4 + I_2 r^3 + I_3 r^2 + I_4 r + I_5 \tag{8}$$

where

$$\begin{aligned}
I_1 &= -\alpha^2 a^2 \frac{a^2 - l^2}{(a^2 + l^2)^2} - \frac{\Lambda}{3}\,, \\
I_2 &= 2\alpha a \left(\alpha a m \frac{a^2 - l^2}{(a^2 + l^2)^2} - \frac{l}{a^2 - l^2} - l \frac{a^2 - l^2}{a^2 + l^2} \frac{\Lambda}{3} \right), \\
I_3 &= 1 + \frac{4\alpha a m l}{a^2 + l^2} - \alpha^2 a^2 \frac{a^2 - l^2}{(a^2 + l^2)^2} (a^2 - l^2 + e^2 + g^2) - (a^2 + 3l^2) \frac{\Lambda}{3}\,, \\
I_4 &= -2m - \frac{2\alpha a l}{a^2 + l^2} (a^2 - l^2 + e^2 + g^2)\,, \\
I_5 &= a^2 - l^2 + e^2 + g^2.
\end{aligned} \tag{9}$$

The roots of the quadratic equation, represented in (8), could be arranged in a range of "maximally four horizons" to "maximally one horizon", for various sub-cases. Considering the most general case (maximally four horizons, $I_1 \neq 0$), including all parameters, provides quite complicated expressions. To this aim, let us express Equation (8) by factoring I_4 as

$$Q(r) = -N(r - r_h^+)(r - r_h^-)(r - r_c^+)(r - r_c^-), \tag{10}$$

where $N = -I_4$, and the outer/inner and cosmo–acceleration horizons are as follows:

$$\begin{aligned}
r_h^{\pm} &= \frac{1}{2}\left(\sqrt{D} + \frac{K}{N} \pm \sqrt{E - \frac{2F}{\sqrt{D}}}\right), \\
r_c^{\pm} &= \frac{1}{2}\left(-\sqrt{D} + \frac{K}{N} \pm \sqrt{E + \frac{2F}{\sqrt{D}}}\right),
\end{aligned} \tag{11}$$

where

$$\begin{aligned}
D &= \frac{K^2}{N^2} + \frac{1}{3N}\left[2X - (Z + i\sqrt{Y^3 - Z^2})^{1/3} - (Z - i\sqrt{Y^3 - Z^2})^{1/3}\right], \\
E &= 3\frac{K^2}{N^2} + \frac{2X}{N} - D\,, \\
F &= -\frac{K^3}{N^3} + \frac{2R}{N} - \frac{KX}{N^2},
\end{aligned} \tag{12}$$

N is indicated as $-I_4$ and the rest of the parameters are given as

$$
\begin{aligned}
K &= \frac{a\alpha}{a^2+l^2}\left[\left(\frac{a\alpha}{a^2+l^2}m - \frac{\Lambda}{3}l\right)(a^2-l^2) - l\right], \\
R &= m + \frac{a\alpha l}{a^2+l^2}(a^2-l^2+e^2+g^2), \\
X &= 1 + \frac{4lam\alpha}{a^2+l^2} - \frac{a^2\alpha^2(a^2-l^2)}{(a^2+l^2)^2}(a^2-l^2+e^2+g^2) - (a^2+3l^2)\frac{\Lambda}{3}, \\
Y &= X^2 + 12KR - 12(a^2-l^2+e^2+g^2)N, \\
Z &= X^3 + 18KRX - 54R^2N + 18(a^2-l^2+e^2+g^2)(3K^2+2NX).
\end{aligned} \tag{13}
$$

In the case of the NRIGP black hole, the metric function $Q(r)$ (Equation (7)) is much simpler than in Equation (3), but is still a fourth-order polynomial with two outer and inner black hole horizons $\tilde{r}_h^{\pm}$ and two outer and inner cosmological horizons $\tilde{r}_c^{\pm}$, in which the symbol of tilde differentiates the corresponding parameters in the NRIGP metric. The metric function for the NRIGP is given by

$$
\tilde{Q}(r) = \tilde{I}_1 r^4 + \tilde{I}_3 r^2 + \tilde{I}_4 r + \tilde{I}_5, \tag{14}
$$

where $\tilde{I}_1 = -\frac{\Lambda}{3}$, $\tilde{I}_2 = 0$, $\tilde{I}_3 = 1 - \Lambda l^2$, $\tilde{I}_4 = -2m$, and $\tilde{I}_5 = e^2 + g^2 - l^2$. The inner and outer horizons of the NRIGP metric are derived as

$$
\tilde{r_h}^{\pm} = \frac{1}{2}\left[-\frac{2\tilde{I}_3}{3\tilde{I}_1} + \frac{H}{6\tilde{I}_1} + \frac{2}{3}\frac{12\tilde{I}_1\tilde{I}_5 + \tilde{I}_3^2}{\tilde{I}_1 H}\right]^{1/2} \pm \left[-\frac{4\tilde{I}_3}{3\tilde{I}_1} - \frac{H}{6\tilde{I}_1} - \frac{2}{3}\frac{12\tilde{I}_1\tilde{I}_5 + \tilde{I}_3^2}{\tilde{I}_1 H}\right]^{1/2}, \tag{15}
$$

and the cosmological horizons

$$
\tilde{r_c}^{\pm} = -\frac{1}{2}\left[-\frac{2\tilde{I}_3}{3\tilde{I}_1} + \frac{H}{6\tilde{I}_1} + \frac{2}{3}\frac{12\tilde{I}_1\tilde{I}_5 + \tilde{I}_3^2}{\tilde{I}_1 H}\right]^{1/2} \pm \left[-\frac{4\tilde{I}_3}{3\tilde{I}_1} - \frac{H}{6\tilde{I}_1} - \frac{2}{3}\frac{12\tilde{I}_1\tilde{I}_5 + \tilde{I}_3^2}{\tilde{I}_1 H}\right]^{1/2}, \tag{16}
$$

which

$$
\begin{aligned}
H = \Bigg[&-288\tilde{I}_5\tilde{I}_3\tilde{I}_1 + 108\tilde{I}_4^2\tilde{I}_1 + 8\tilde{I}_3^3 + 12\tilde{I}_1 \times \\
&\sqrt{\frac{-3}{\tilde{I}_1}\left(256\tilde{I}_1^2\tilde{I}_5^3 - 128\tilde{I}_1\tilde{I}_3^2\tilde{I}_5^2 + 144\tilde{I}_1\tilde{I}_3\tilde{I}_4^2\tilde{I}_5 - 27\tilde{I}_1\tilde{I}_4^4 + 16\tilde{I}_3^4\tilde{I}_5 - 4\tilde{I}_3^3\tilde{I}_4^2\right)}\Bigg]^{1/3}.
\end{aligned} \tag{17}
$$

The acceleration parameter a in the main metric Equation (1) contains the ergoregion with the boundary of $g_{tt} = 0$ and written by $Q(r_e) = P(\theta)a^2 sin^2\theta$. In the NRIGP case, there is no acceleration parameter $a \neq 0$; thus, there is no ergoregion.

3. Scalar Perturbation

In this section, we focus on the scalar perturbation of the NRIGP black hole. To this aim, the massive Klein–Gordon equation is applied, which describes the dynamics of the particle in quantum field theory [32,33]. The Klein–Gordon equation describes the relativistic wave equation of the Schrödinger equation for zero-spin particles (scalar particles). The massive Klein–Gordon equation is given by

$$
\frac{1}{\sqrt{-g}}D_\mu\left[\sqrt{-g}g^{\mu\nu}D_\nu\right]\Psi = \mu_0, \tag{18}
$$

where μ_0 and g are the mass of the particles and metric tensor determinant of the NRIGP line element (in Equation (6)), respectively; thus, $\sqrt{-g} = (r^2 + l^2)\sin\theta$. Also,

$$D_\mu = \partial_\mu - iqA_\mu \tag{19}$$

Here, q is the charge of the scalar particles and A_μ indicates the vector potential of the NRIGP black hole which has two components A_t and A_ϕ, defined as

$$A = -\frac{er + gl}{r^2 + l^2}dt + \frac{(er + gl)4lsin^2\frac{1}{2}\theta + g(r^2 + l^2)cos\theta}{r^2 + l^2}d\phi. \tag{20}$$

Furthermore, the metric tensor of Equation (6) is derived as

$$g_{\mu\nu} = \begin{pmatrix} -\frac{Q}{\rho^2} & 0 & 0 & 4l\frac{Q}{\rho^2}sin^2\frac{1}{2}\theta \\ 0 & \frac{\rho^2}{Q} & 0 & 0 \\ 0 & 0 & \frac{\rho^2}{P} & 0 \\ 4l\frac{Q}{\rho^2}sin^2\frac{1}{2}\theta & 0 & 0 & -\frac{b}{\rho^2} \end{pmatrix}, \tag{21}$$

where $b = 16Ql^2sin^4\frac{1}{2}\theta - P\sin^2\theta(r^2 + l^2)^2$. In addition, the inverse of the metric tensor is

$$g^{\mu\nu} = \begin{pmatrix} \frac{b}{QP\rho^2sin^2\theta} & 0 & 0 & \frac{4lsin^2\frac{1}{2}\theta}{P\rho^2sin^2\theta} \\ 0 & \frac{Q}{\rho^2} & 0 & 0 \\ 0 & 0 & \frac{P}{\rho^2} & 0 \\ \frac{4lsin^2\frac{1}{2}\theta}{P\rho^2sin^2\theta} & 0 & 0 & \frac{1}{P\rho^2sin^2\theta} \end{pmatrix}. \tag{22}$$

We substitute Equations (19)–(22) into the Klein–Gordon equation, also introducing an ansatz as

$$\Psi(r, t) = R(r)S(\theta)e^{i\bar{m}\phi}e^{-i\omega t}, \tag{23}$$

where $\bar{m}$ denotes the azimuthal number and ω is the frequency of the spinor fields, to reach

$$\frac{2rQ}{\rho^2R(r)}\partial_rR(r) + \rho^2\partial_r(\frac{Q}{\rho^2})\frac{\partial_rR(r)}{R(r)} + \frac{Q}{R(r)}\partial_r^2R(r) + P\cot\theta\frac{\partial_\theta S(\theta)}{S(\theta)} + P\frac{\partial_\theta^2S(\theta)}{S(\theta)} - \frac{1}{Psin^2\theta}\times \left[\bar{m} - qgcos\theta - 4lsin^2\frac{1}{2}\theta\omega\right]^2 + \frac{\rho^4}{Q}(\omega + qA_t)^2 = \mu_0\rho^2. \tag{24}$$

We separate the radial and angular parts in Equation (24) and apply a new transformation $R(r) = \frac{U(r)}{\sqrt{r^2+l^2}}$, to find the following radial expression:

$$\rho^2\partial_r(\frac{Q}{\rho^2}\partial_rU(r)) + \left(\frac{3r^2Q}{(r^2 + l^2)^2} - \frac{Q + rQ'}{(r^2 + l^2)} + \frac{\rho^4}{Q}(\omega + qA_t)^2 - \mu_0\rho^2 - \lambda\right)U(r) = 0, \tag{25}$$

where λ represents the angular part, also, $'$ indicates $\frac{d}{dr}$.

In this step, a new set of coordinates is required, known as the tortoise coordinate r_* or the Regge–Wheeler radial coordinate, which is required to cover the spacetime on the farther side of the horizon r_h and holds everywhere [34,35]. The tortoise coordinate is defined as $dr_* = \frac{dr}{f(r)}$, in which $f(r)$ is a metric function, and for the NRIGP metric it is $dr_* = -\frac{\rho^2}{Q}dr$. In this way, the region $r_h < r < \infty$ is mapping to a greater region (out of the black hole geometry) as $-\infty < r_* < +\infty$ in the tortoise coordinate.

Thus, by applying the tortoise coordinate, the $1-d$ Schrödinger form equation appears as

$$\frac{d^2U(r)}{dr_*} + \left(\omega^2 - V_{eff}\right)U(r) = 0, \tag{26}$$

where V_{eff} represents the effective potential (the radial potential of a $1-d$ separable differential equation):

$$V_{eff} = \frac{Q^2 + rQ'Q}{\rho^6} - \frac{3r^2Q^2}{\rho^8} + \mu_0\frac{Q}{\rho^2} + \frac{\lambda Q}{\rho^4} - (qA_t)^2 - 2\omega q A_t. \tag{27}$$

The effective potential in the black hole framework of the study is a remarkable concept. For a nonrotating black hole, the effective potential V_{eff} comprises two essential gravitational and centrifugal forces. Thus, instead of evaluating each force individually, we can predict the black hole behavior by considering the effective potential, which includes both forces.

However, it has been shown that certain perturbations on the horizon of black holes would affect the instability of the geometry, even at the classical level. Since the potential is characterized by asymptotically flat spacetimes, the expected form of the effective potential is Gaussian-like shapes. The deviation from this normal shape could be interpreted as a significant effect on spacetime geometry. On the other hand, its relation with greybody radiation could reveal the probability of particles tunneling in addition to the hopping over of the particles from the potential peak. The depicted figures show the behavior of the effective potential under the influence of different parameters, allowing for a better perspective. Figures are illustrated for both $\Lambda > 0$ (solid lines) and $\Lambda < 0$ (dotted lines). The graphs in Figure 2 show the behavior of the effective potential by changing the magnetic charge g (left) and the electric charge e (right).

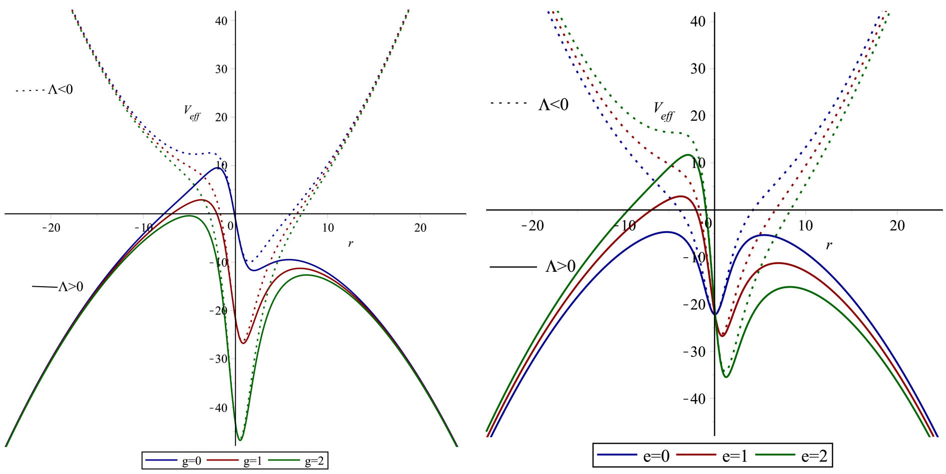

Figure 2. Effective potentials of the NRIGP black hole for various magnetic charge parameters g (**left**) and electric charge e (**right**). The solid lines indicate the changes for $\Lambda > 0$ and dotted lines for $\Lambda < 0$. The following parameters are considered as: $q = 0, \omega = 10, l = 2, \lambda = 2$, and $\Lambda = \pm 0.3$.

As shown in Figure 2, the effective potential has almost the same behaviors under changes of g and e, decreasing the peaks and immediately through damping (solid)/rising (dotted) for region $r > 0$ by increasing the indicated parameters. In the $r < 0$ region, by increasing the magnetic charge g, the effective potential also decreases the same as in the $r > 0$ region, but the increase in the electric charge e in the $r < 0$ region causes growth of the picks and shows an inverse behavior.

The graphs in Figure 3 illustrate the effective potential for different NUT parameters l (left) and the cosmological constant Λ (right). When $l = 0$, there is a disconnect between the $r > 0$ and $r < 0$ regions for both $\pm\Lambda$, and the peaks disappear smoothly by increasing the NUT parameter. Moreover, the $\Lambda = 0$ case (dashed line) shows a different form of the effective potential (tends to zero at $\pm\infty$); then, by a small increase in Λ, a sharp damping, and increase appear for $\Lambda > 0$ and $\Lambda < 0$, respectively.

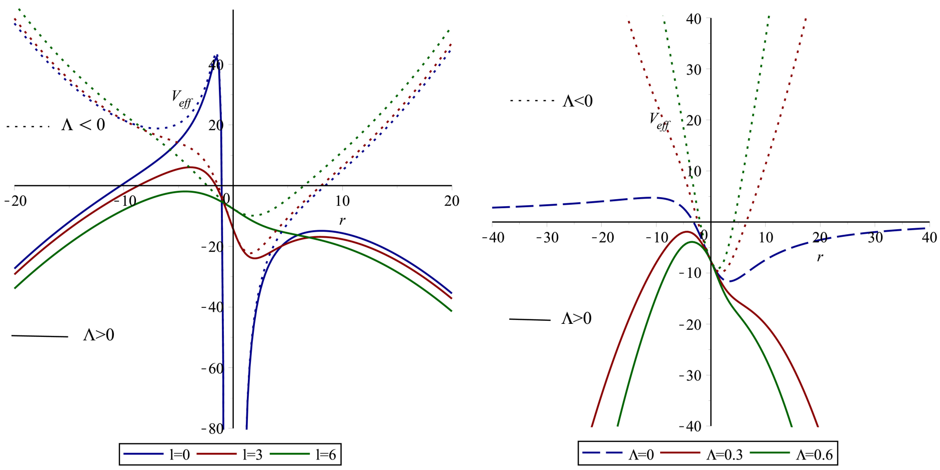

Figure 3. Effective potential of the NRIGP black hole for various NUT parameters l (**left**) and cosmological constant Λ (**right**). The solid lines indicate $\Lambda > 0$ and the dotted ones $\Lambda < 0$. The constant arguments are considered as; $e = q = 2, g = 1, \omega = 10$, and $\lambda = 2$.

4. Scalar Greybody Factor of NRIGP Black Hole

Greybody factor/transmission probability, also known as absorption cross-section, is a frequency-dependent parameter $\sigma(\omega)$, representing the possibility of reaching Hawking radiation to infinity. The journey for the escaped particles from the event horizon is challenging because the spacetime around the black hole behaves as a potential barrier for them.

From the observer at infinity, the escaping radiation spectrum is thermal, with a temperature of $T_H = \frac{\hbar}{K_B 8\pi M}$ [1]. The total number of the particles is emitted in the mode n with frequency ω given by [36]

$$N_n(\omega) = \frac{|T_n(\omega)|^2}{\left(e^{\frac{\hbar\omega}{K_B T_H}} \mp 1\right)}, \tag{28}$$

where the "$-$" sign represents bosons (spinless particles) and the "$+$" sign represents fermions (spin half particles), and $T_n(\omega)$ represents the transmission probability.

In this study, we apply a semianalytic method that provides a general rigorous bound in the transmission probability for the one-dimensional potential scattering [37–39]. The general bound equation for the greybody factor is given by

$$\sigma(\omega) \geq \sec h^2\left(\int_{-\infty}^{+\infty} \wp dr_*\right), \tag{29}$$

where $\wp$ is defined as

$$\wp = \frac{\sqrt{(F')^2 + (\omega^2 - V_{eff} - F^2)^2}}{2F}. \tag{30}$$

Here, F is a positive function with two conditions: (1) $F(r_*) > 0$ and (2) $F(+\infty) = F(-\infty) = \omega$. Direct substitution of the effective potential derived in Section 3 in

Equation (27) gives an undefined result for the greybody factor. In this regard, without losing generality, we can set $F^2 = \omega^2 - V_{eff}^2$ in Equation (30). Thus, Equation (29) is written by

$$\sigma(\omega) \geq \sec F^2 \left(\frac{1}{2} \int_{-\infty}^{+\infty} |\frac{F'}{F}| dr_* \right). \tag{31}$$

The result in parentheses after integration is $\ln(\frac{F_{peak}}{F})$; thus, Equation (31) changes to

$$\sigma(\omega) \geq \frac{4\omega^2(\omega^2 - V_{peak})}{(2\omega^2 - V_{peak})^2}. \tag{32}$$

In order to derive V_{peak} in Equation (32), we first determine the r_{peak} by taking the derivative from the effective potential of Equation (27). The direct results of Equation (32) are illustrated in Figures 4 and 5. The greybody factor graphs are depicted for negative cosmological constant $\Lambda < 0$ (dotted lines) and positive $\Lambda > 0$ (solid lines) for various parameters such as "e, g, l, and Λ". Depicted in Figure 4 are the behavior of the greybody factor of the NRIGP black hole under the varying of the electric charge "e" (left figure) and magnetic charge "g" (right figure) parameters. The greybody factor is between zero and one, and the closest graph to one means the highest probability of reaching infinity; thus, the case of $e = 0$ in $\Lambda < 0$ has the highest transmission probability. By raising both electric and magnetic charges e and g, respectively, the NRIGP greybody factor starts to decrease in $\Lambda < 0$, but by increasing the magnetic charge "g" the greybody radiation also increases very smoothly.

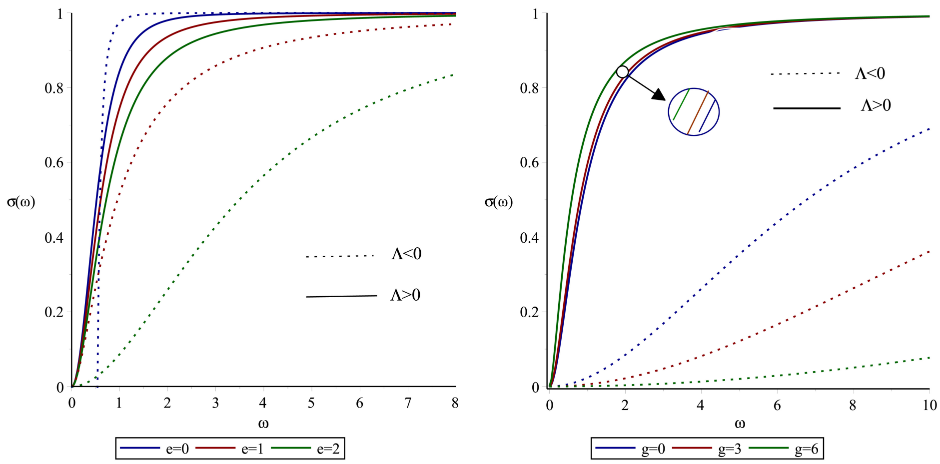

Figure 4. The NRIGP greybody factor under the impression of the electric charge e (**left**) and magnetic charge g (**right**). The solid lines are depicted for $\Lambda > 0$, and dotted ones are shown for $\Lambda < 0$. The constant parameters are considered as follows: $l = 0.1, \Lambda = \pm 0.3, l = 0.1, q = 1.5$, and $\lambda = 2$.

The graphs in Figure 5 show the NRIGP greybody factor under the influence of the NUT parameter l (left) and the cosmological constant Λ (right). The consistency between the effective potential and the greybody factor could explain the behavior of the greybody factor under the variation of the NUT parameter for the $\Lambda < 0$ case. The high potential barriers for different cosmological constants, shown in Figure 3, could be the reason for the disorganized (for $\Lambda > 0$) and very low transmission probability for variation in positive and negative Λ.

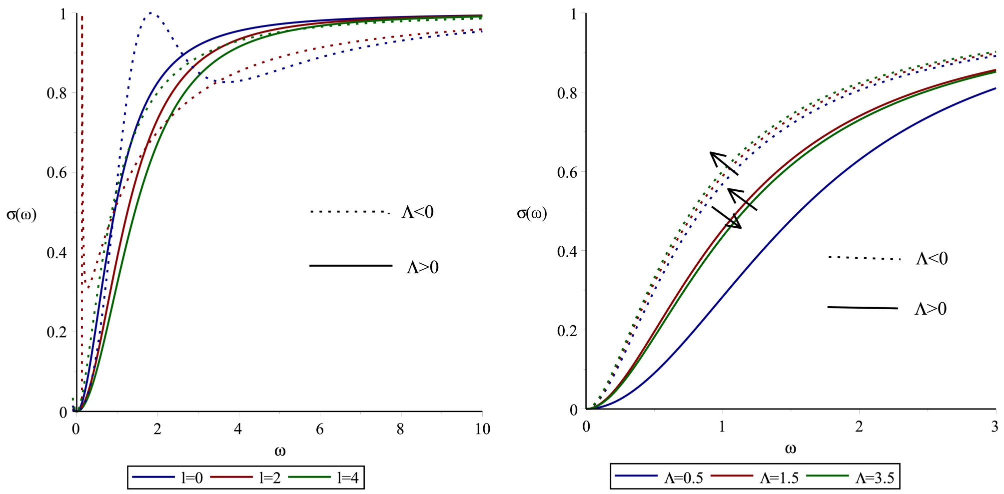

Figure 5. The NRIGP greybody factor under the impression of the NUT parameter l (**left**) and cosmological constant Λ (**right**). The solid lines are depicted for $\Lambda > 0$, and dotted ones are shown for $\Lambda < 0$. The arrow in the dotted graph (right) means increasing and the arrows in the solid ones indicate the greybody factor increase by increasing Λ then after $\Lambda = 1.5$ it starts to decrease. The constant parameters are as follows: $g = e = 3, q = 1.5$, and $\lambda = 2$.

In order to have a clear perspective, we can also refer to the same investigations of the exact black hole solutions as Schwarzschild and Reissner-Nordström [40–42] (i.e., in Ref. [40] the greybody factors of the Schwarzschild black hole for different models are shown. Also, refer to [41] for the effective potentials, and the behavior of the greybody factor in the Reissner–Nordström–de Sitter black hole).

5. Conclusions

In this paper, we studied the greybody factor from a more general perspective for a metric that includes the most important factors of a black hole altogether. To this aim, we applied the nonrotating of the improved Griffiths–Podolsk metric and called it the "NRIGP" metric. As is mentioned in Equation (1), the original form of the improved Griffiths–Podolsk metric contains the electric and magnetic charges "e" and "g", respectively, NUT "l", Kerr "a", and acceleration "α" parameters, and also the cosmological constant "Λ". In this study, we consider the nonrotating $(a = 0)$ and, consequently, the nonacceleration $(\alpha = 0)$ form of the metric, as represented in Equation (6).

Since Hawking claimed that black holes can emit as well as absorb particles, many promising investigations have improved in this area [43–47]. The mentioned parameters are all evaluated for different black hole thermodynamical aspects and greybody radiation in separate studies [7,16,48,49]; thus, the evaluation of the combination in one structure is missing in the literature and might be functional in different physical aspects of the black hole.

The scalar perturbation is evaluated in Section 3 by utilizing the massive and charged Klein–Gordon Equation (18) to derive the effective potential Equation (27) from the one-dimensional Schrödinger like Equation (26). The potential around a black hole, which is identical to the regarded spacetime, makes an essential impact on the greybody radiation as it behaves as a barrier for the particles that had a chance to escape; if those particles are not bound back to the black hole, they can be considered greybody radiation. Figures 2 and 3 show the action of the effective potential by varying the electric and magnetic charges "e" and "g", respectively, the NUT parameter "l", and the cosmological constant Λ.

In the current study, greybody factors are affected by the maximum value of effective potentials within a given specific field. It is expected that for the smaller peaks of the effective potential, a fixed-energy particle includes a higher transmission probability, which means that the greybody factor increases. Thus, the comparison between the figures indicated that the most normal actions belong to an increase in negative Λ and "g". As illustrated in Figure 3 (right), in comparison to other parameters, there is a significant difference between $\Lambda = 0$ and $\Lambda \neq 0$, and this bizarre behavior also affects the greybody factor.

The semianalytic method for defining the greybody factor/transmission probability represented in Equations (29) and (30) involved undefined terms to make the process fail. In order to solve the problem, instead of considering $F = \omega$ in Equation (30), we plugged in $F^2 = \omega^2 - V_{eff}^2$; in this way, the integral limitations are not contemplated, and undefined terms are vanishing. We derived the greybody factor of the NRIGP metric from Equation (32). First, the v_{peak} should be set by deriving the r_{peak}, which is a long computation. Therefore, the direct result of Equation (32) for parameters "e, g, l, Λ" are depicted in Figures 4 and 5.

We can conclude that, in the NRIGP spacetime, the approach of the effective potential to infinity is very slow because there are nonzero effective parameters such as Λ, e, g, and l in the evaluation of each case. Moreover, the results of this study reveal that the indicated parameters gathering in one black hole may strongly affect the black hole spacetime geometry, while in the individual investigation, the effect would be unconvincing. It is shown that by increasing parameters like the magnetic charge "g", the effective potential becomes less intense, allowing the particles to escape more easily from the event horizon than when the electric charge e and NUT parameter l increase.

Funding: This research received no external funding.

Data Availability Statement: No new data were created or analyzed in this study.

Conflicts of Interest: The author declares no conflicts of interest.

References

1. Hawking, S.W. Particle creation by black holes. *Commun. Math. Phys.* **1975**, *43*, 199. [CrossRef]
2. Hawking, S.W. Black Holes and Thermodynamics. *Phys. Rev. D* **1976**, *13*, 191. [CrossRef]
3. Boonserm, P.; Chatrabhuti, A.; Ngampitipan, T.; Visser, M. Greybody factors for Myers-Perry black holes. *J. Math. Phys.* **2014**, *55*, 112502. [CrossRef]
4. Hyun, Y.H.; Kim, Y.; Park, S.C. Exact Greybody Factors for the Brane Scalar Field of Five-dimensional Rotating Black Holes. *J. High Energy Phys.* **2019**, *6*, 041. [CrossRef]
5. Jorge, R.; de Oliveira, E.S.; Rocha, J.V. Greybody factors for rotating black holes in higher dimensions. *Class. Quant. Grav.* **2015**, *32*, 065008. [CrossRef]
6. Sharif, M.; Ama-Tul-Mughani, Q. Greybody factor for quintessential Kerr–Newman black hole. *Phys. Dark Univ.* **2020**, *27*, 100436. [CrossRef]
7. Al-Badawi, A.; Kanzi, S.; Sakallı, İ. Fermionic and bosonic greybody factors as well as quasinormal modes for charged Taub NUT black holes. *Ann. Phys.* **2023**, *452*, 169294. [CrossRef]
8. Kanzi, S.; Sakallı, İ. Greybody radiation and quasinormal modes of Kerr-like black hole in Bumblebee gravity model. *Eur. Phys. J. C* **2021**, *81*, 501. [CrossRef]
9. Uniyal, A.; Kanzi, S.; Sakallı, İ. Some observable physical properties of the higher dimensional dS/AdS black holes in Einstein-bumblebee gravity theory. *Eur. Phys. J. C* **2023**, *83*, 668. [CrossRef]
10. Kanzi, S.; Mazharimousavi, S.H.; Sakallı, İ. Greybody factors of black holes in dRGT massive gravity coupled with nonlinear electrodynamics. *Ann. Phys.* **2020**, 422, 168301. [CrossRef]
11. Boonserm, P.; Phalungsongsathit, S.; Sansuk, K.; Wongjun, P. Greybody factors for massive scalar field emitted from black holes in dRGT massive gravity. *Eur. Phys. J. C* **2023**, *83*, 657. [CrossRef]
12. Sakallı, İ.; Kanzi, S. Physical properties of brane-world black hole solutions via a confining potential. *Ann. Phys.* **2022**, *439*, 168803. [CrossRef]
13. Maldacena, J.M.; Strominger, A. Black hole grey body factors and d-brane spectroscopy. *Phys. Rev. D* **1997**, *55*, 861–870. [CrossRef]
14. Karmakar, R.; Goswami, U.D. Quasinormal modes, thermodynamics and shadow of black holes in Hu–Sawicki $f(R)$ gravity theory. *Eur. Phys. J. C* **2024**, *84*, 969. [CrossRef]

15. Oshita, N.; Takahashi, K.; Mukohyama, S. Stability and instability of the black hole greybody factors and ringdowns against a small-bump correction. *Phys. Rev. D* **2024**, *110*, 084070. [CrossRef]
16. Fatima, G.; Shaukat, S.; Javed, F.; Mustafa, G. Greybody factors, quasi-normal modes and thermal fluctuations of quantum-corrected Schwarzschild black hole surrounded by quintessence. *Phys. Dark Univ.* **2024**, *45*, 101521. [CrossRef]
17. Okabayashi, K.; Oshita, N. Greybody factors imprinted on black hole ringdowns. II. Merging binary black holes. *Phys. Rev. D* **2024**, *110*, 064086. [CrossRef]
18. Lin, J.; Bravo-Gaete, M.; Zhang, X. Quasinormal modes, greybody factors, and thermodynamics of four dimensional AdS black holes in critical gravity. *Phys. Rev. D* **2024**, *109*, 104039. [CrossRef]
19. Kanzi, S.; Sakallı, İ.; Pourhassan, B. Superradiant (In)stability, Greybody Radiation, and Quasinormal Modes of Rotating Black Holes in Non-Linear Maxwell f(R) Gravity. *Symmetry* **2023**, *15*, 873 . [CrossRef]
20. Jha, S.K. Photonsphere, shadow, quasinormal modes, and greybody bounds of non-rotating Simpson–Visser black hole. *Eur. Phys. J. Plus* **2023**, *138*, 757. [CrossRef]
21. Yang, Z.H.; Lei, Y.H.; Kuang, X.M.; Wu, J.P. Perturbations of massless external fields in a special Horndeski hairy black hole. *Eur. Phys. J. C* **2024**, *84*, 153. [CrossRef]
22. Bunjusuwan, S.; Chen, C.H. The greybody factor for the monopole and odd-parity modes of the Proca field in the Schwarzschild black hole spacetimes. *J. Phys. Conf. Ser.* **2023**, *2653*, 012022. [CrossRef]
23. Oshita, N. Thermal ringdown of a Kerr black hole: Overtone excitation, Fermi-Dirac statistics and greybody factor. *J. Cosmol. Astropart. Phys.* **2023**, *4*, 13. [CrossRef]
24. Podolsky, J.; Vratny, A. New improved form of black holes of type D. *Phys. Rev. D* **2021**, *104*, 084078. [CrossRef]
25. Podolsky, J.; Vratny, A. New form of all black holes of type D with a cosmological constant. *Phys. Rev. D* **2023**, *107*, 084034; Erratum in *Phys. Rev. D* **2023**, *108*, 129902. [CrossRef]
26. Debever, R. On type D expanding solutions of Einstein–Maxwell equations. *Bull. Soc. Math. Belg.* **1971**, *23*, 360–376.
27. Plebanski, J.F.; Demianski, M. Rotating, charged and uniformly accelerating mass in general relativity. *Ann. Phys.* **1976**, *98*, 98–127. [CrossRef]
28. Griffiths, J.B.; Podolsky, J. Accelerating and rotating black holes. *Class. Quant. Grav.* **2005**, *22*, 3467–3480. [CrossRef]
29. Ovcharenko, H.; Podolsky, J.; Astorino, M. Black holes of type D revisited: Relating their various metric forms. *arXiv* **2024**, arXiv:2409.02308.
30. Podolsky, J.; Griffiths, J.B. Accelerating Kerr-Newman black holes in (anti-)de Sitter space-time. *Phys. Rev. D* **2006**, *73*, 044018. [CrossRef]
31. Griffiths, J.B.; Podolsky, J. A New look at the Plebanski-Demianski family of solutions. *Int. J. Mod. Phys. D* **2006**, *15*, 335–370. [CrossRef]
32. Alfimov, G.L.; Kevrekidis, P.G.; Konotop, V.V.; Salerno, M. Wannier functions analysis of the nonlinear Schrödinger's equation with a periodic potential. *Phys. Rev. E* **2002**, *66*, 046608. [CrossRef] [PubMed]
33. Bawin, M.; Jaminon, M. Pion Form-Factor And The Klein-Gordon Equation. *Phys. Rev. C* **1984**, *30*, 331–334. [CrossRef]
34. Liu, X.; Zhao, Z.; Liu, W. Tortoise coordinate transformation on apparent horizon of a dynamical black hole. *Int. J. Mod. Phys. Conf. Ser.* **2012**, *12*, 358–367. [CrossRef]
35. Gui-hua, T.; Wang, S.k.; Zhong, S. The Effect of the tortoise coordinate on the stable study of the Schwarzschild black hole. *arXiv* **2006**, arXiv:gr-qc/0603113.
36. Andersson, N.; Jensen, B.P. Scattering by Black Holes. Chapter 0.1. *arXiv* **2006**, arXiv:gr-qc/0011025.
37. Visser, M. Some general bounds for 1-D scattering. *Phys. Rev. A* **1999**, *59*, 427–438. [CrossRef]
38. Boonserm, P.; Visser, M. Bounding the Bogoliubov coefficients. *Ann. Phys.* **2008**, *323*, 2779–2798. [CrossRef]
39. Boonserm, P.; Visser, M. Transmission probabilities and the Miller-Good transformation. *J. Phys. A* **2009**, *42*, 45301. [CrossRef]
40. Gray, F.; Visser, M. Greybody Factors for Schwarzschild Black Holes: Path-Ordered Exponentials and Product Integrals. *Universe* **2018**, *4*, 93. [CrossRef]
41. Ahmed, J.; Saifullah, K. Greybody factor of a scalar field from Reissner–Nordström–de Sitter black hole. *Eur. Phys. J. C* **2018**, *78*, 316. [CrossRef]
42. Ngampitipan, T.; Boonserm, P. Bounding the greybody factors for the Reissner-Nordström black holes. *J. Phys. Conf. Ser.* **2013**, *435*, 012027. [CrossRef]
43. Xin, Z.; Wei, X. Hawking–Page transition and the dual relations of anti-de Sitter black holes surrounded by dark energy in general dimensions. *Commun. Theor. Phys.* **2024**, *76*, 075403. [CrossRef]
44. Lin, S.Y.; Yu, M.H.; Ge, X.H.; Tian, L.J. Entanglement entropy, phase transition, and island rule for Reissner-Nordström-AdS black holes *Phys. Rev. D* **2024**, *110*, 4. [CrossRef]
45. Corda, C.; Cafaro, C. Universality of the thermodynamics of a quantum-mechanically radiating black hole departing from thermality. *Phys. Lett. B* **2024**, *856*, 138948. [CrossRef]

46. Ghaffari, S.; Luciano, G.G.; Sheykhi, A. Nonextensive entropies impact onto thermodynamics and phase structure of Kerr–Newman black holes. *Phys. Dark Univ.* **2024**, *44*, 101447. [CrossRef]
47. Khosravipoor, M.R.; Farhoudi, M. Thermodynamics of deformed AdS-Schwarzschild black hole. *Eur. Phys. J. C* **2023**, *83*, 1045. [CrossRef]
48. Upadhyay, S.; Mandal, S.; Myrzakulov, Y.; Myrzakulov, K. Weak deflection angle, greybody bound and shadow for charged massive BTZ black hole. *Ann. Phys.* **2023**, *450*, 169242. [CrossRef]
49. Javed, W.; Aqib, M.; Övgün, A. Bounding greybody and deflection angle of improved Schwarzschild black hole. *New Astron.* **2022**, *96*, 101827. [CrossRef]